Fluorescence ($^4T_2 \rightarrow {}^4A_2$) and phosphorescence ($^2E \rightarrow {}^4A_2$) in MgO:$Cr^{3+}$†

Francesco Castelli* and Leslie S. Forster

Department of Chemistry, University of Arizona, Tucson, Arizona 85721

(Received 15 August 1974)

Steady-state and time-resolved spectra have been recorded for MgO:Cr^{3+} crystals as a function of temperature, excitation wavelength, and Cr^{3+} concentration. The spectra and lifetimes for emission from the various centers have been determined. Both prompt and delayed broad-band fluorescence are emitted, but only delayed fluorescence is associated with the cubic and tetragonal sites. The thermal quenching mechanism of the R-line lifetime is reconsidered and shown to involve repopulation of the $^4T_2$ state. For the cubic and tetragonal centers $^4T_2$ is above ^2E, the $^4T_2$ lifetime < 0.5 nsec and the $^4T_2 \rightarrow {}^2E$ intersystem crossing efficiency is unity. For the rhombic centers, where $^4T_2$ is below ^2E, the $^4T_2$ lifetime is 35 μsec. The total luminescence quantum yields for all centers is close to unity.

I. INTRODUCTION

The emission of MgO:Cr^{3+} consists of sharp lines superimposed upon a broad band.[1] The line at 6981 Å (R line) has been assigned as the magnetic dipole no-phonon $^2E \rightarrow {}^4A_2$ transition arising from Cr^{3+} in cubic sites.[2] $^2E \rightarrow {}^4A_2$ emission lines from Cr^{3+} in noncubic sites (N lines) have been assigned as follows: 6992 and 7038 Å, no-phonon transitions arising from Cr^{3+} with a vacancy in the [100] direction; 6989 and 7035 Å, due to Cr^{3+}-vacancy-Cr^{3+} clusters in the [100] direction.[3,4] These sites are designated as single-ion tetragonal and pair-tetragonal centers, respectively. There are also Cr^{3+}-vacancy sites with the vacancy in the [110] direction. Emission from these rhombic sites has not been definitely identified.[4] In addition to the no-phonon lines there are vibronic sidebands associated with the R and N lines. The intensities of both sets of N lines relative to the R line increase with Cr^{3+} concentration, but the concentration dependence of the pair-tetragonal intensities is the more pronounced.

A broad fluorescence band whose intensity increases with Cr^{3+} concentration was described by Imbusch.[5] This band, with a maximum near 800 nm, was examined in greater detail by Parker *et al.*[1] who assigned it as $^4T_2 \rightarrow {}^4A_2$ from cubic site Cr^{3+}. The lifetime of this emission is less than 100 μsec, while the R-line lifetime varies from 11.6 msec (77°K) to ~2 msec (300°K).[5] The double lifetime is consistent with dual emission from cubic site Cr^{3+}, i.e., prompt $^4T_2 \rightarrow {}^4A_2$ fluorescence, and $^2E \rightarrow {}^4A_2$ phosphorescence. However, the different variation of the broad-band and R-line intensities with Cr^{3+} concentration is inconsistent with this interpretation. This work was initiated to obtain more information about the origin of the broad-band emission and to gain insight into the relationship between the $^4T_2$-state lifetime and the $^4T_2 - {}^2E$ separation.

II. EXPERIMENTAL METHODS

For steady-state emission and excitation spectral measurements, excitation was obtained with a 0.25-m Bausch and Lomb monochromator and PEK lamps (100-W Hg and 75-W Xe). Emission at 90° was passed through a 0.25-m Jarrell-Ash monochromator, and detected by a dry-ice-cooled red-extended S-20 Centronic (Q42835A) photomultiplier tube. Unless specified otherwise, 0.5-mm slits (1.7-nm bandwidth) were used on the emission monochromator. The signal was d.c. amplified and recorded. Separate excitation spectra were recorded for the R ($\lambda = 6981$ Å) and N lines, but the two N lines at 7035 and 7038 Å were not resolvable. Excitation spectra were corrected by calibration against a Rhodamine B solution quantum counter and a calibrated United Detector Technology PIN 10D solid-state photodiode.

The Cr^{3+} MgO: crystals were mounted in a vacuum on the copper coldfinger of a Hoffman Dewar for the 77°K measurements.

In recording excitation spectra as a function of emission wavelength, the position of the crystal was not altered. This ensures the reliability of all qualitative conclusions based upon a comparison of the excitation spectra for different emission wavelengths. The high-resolution emission spectra were recorded at 90° by passing the lamp excitation through the 0.25-m Jarrell-Ash monochromator and scanning the emission with a 0.75-m Jarrell-Ash Czerny-Turner monochromator. The emission was modulated and the signal from an E.M.I. 9558QA S-20 photomultiplier detected with a lock-in amplifier.

Emission decays were excited either with a N_2

pulsed laser (Avco C950) or with N_2 laser-pumped PBD or Rhodamine-6G dye lasers. The corresponding exciting wavelengths were 337, 366, and 580 nm, respectively. The PBD dye laser was untuned with a 3-nm bandwidth; the Rhodamine-6G dye laser was tuned at 580 nm with a bandwidth of less than 1 nm in order to minimize interference from scattered excitation light. The pulse width was always shorter than 10 nsec. For the 77°K measurements a Pyrex Dewar was used, and the crystal was cooled by immersion in liquid nitrogen. The emission at 90° was filtered by 5 cm of a concentrated chromium acetylacetonate solution to reduce scattered excitation light, and focused onto the slit of the 0.25-m Jarrell-Ash monochromator. The chromium acetylacetonate solution absorbed some of the shorter wavelength emission and induced a slight distortion of the emission spectra. The Centronic photomultiplier, wired for fast response, was used for most of the pulsed measurements. However, where indicated, a RCA C-31034 photomultiplier with an almost constant sensitivity up to 900 nm was used as the detector. This photomultiplier is faster but has less gain than the Centronic tube and yields spectra that are almost "corrected." The photomultiplier load resistors were varied from 50 Ω to 1 MΩ, as required by the desired response time and spectral resolution. The photomultiplier output was fed to a 7904 Tektronix oscilloscope with a 7A19 or 7A11 amplifier. For lifetime measurements the scope trace was photographed. Time-resolved spectra were obtained by scanning the emission spectrum and processing the scope output with a PAR Model 60 Box Car Integrator at different delay times. Most of the work was performed with single crystals kindly given to us by Imbusch, who determined the concentrations of the various centers of the more concentrated sample by ESR measurement as: cubic, 7×10^{18} cm^{-3}; tetragonal, 1.3×10^{18} cm^{-3}; rhombic, 0.3×10^{18} cm^{-3}. The Cr^{3+} concentration in the dilute sample was smaller than the above by an order of magnitude. All of the results shown in the figures were obtained with this sample. Results were checked with single crystals of nominal concentration 1×10^{20} and 1.5×10^{19} cm^{-3} obtained from Norton Research Corp. (Canada) Ltd.

III. RESULTS

Steady-state emission spectra

Emission spectra from the dilute MgO:Cr^{3+} crystal have been recorded at different excitation wavelengths (297, 313, 366, 404, 436, 500, 546, and 577 nm) at room temperature (~296°K) and 77°K. Representative spectra are shown in Figs. 1 and 2. A variation of the emission spectrum with excitation wavelength is evident and the near concordance of spectra excited at 436 and 600 nm (Ref. 1) does

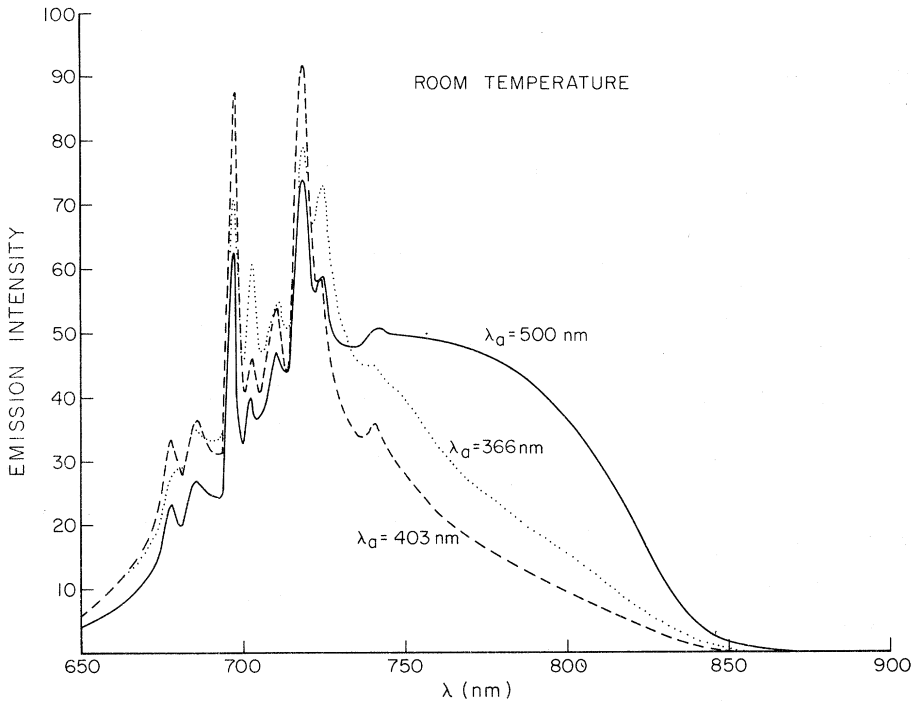

FIG. 1. Room-temperature steady-state emission spectra of MgO:Cr^{3+} (Cr^{3+} < 10^{18} cm^{-3}) at different excitation wavelengths (λ_a).

not extend to other excitation wavelengths. The relative intensities of the R and N lines with the associated vibrational structure are a function of the fraction of incident light absorbed by the cubic and the tetragonal centers, respectively. The intensities at 698, 711, 718, and 741 nm rise and fall together. Hence, the 711-, 718-, and 741-nm features can be assigned as vibrational sidebands of the R line and arise from cubic sites. The 725-nm band appears to be associated with the 704-nm line, but the intensity variation of the broad band peaked at 780 nm does not follow either the 698- or 704-nm line intensity changes. The 731-nm line and the broad-band intensities appear to be related.

Increasing the Cr^{3+} concentration in the range 10^{18}–10^{19} cm^{-3} leads to an intensification of the broad band relative to the R and N lines for every excitation wavelength, in contrast with the results of Parker *et al.*[1]

The temperature dependence of the emission spectra is noteworthy. The intensity of the broad band relative to the R and N lines increases with temperature.

The 77°K excitation spectra obtained by monitoring the 698-, 704- and 800-nm emissions are displayed in Fig. 3. The two N lines at 7035 and 7038 Å were not resolved, but excitation spectra for these two lines have been published and they are very similar. In fact, the excitation spectra for 6981, 7035, and 7038 Å emission differ little in the region of $^4T_2 \leftarrow {}^4A_2$ absorption.[6] However, both the $^4T_2 \leftarrow {}^4A_2$ and $^4T_1 \leftarrow {}^4A_2$ excitation bands for the broad fluorescence (monitored at 800 nm) are markedly red shifted relative to the excitation spectra for the structured emission, with the $^4T_2 \leftarrow {}^4A_2$ maximum near 650 nm rather than at 600 nm.

77°K emission spectra at high resolution have been obtained at different excitation wavelengths (Fig. 4). Excitation at 313 nm yields a new emission line at 7031 Å, the same position where a line has been observed in absorption but not in emission.[4] This line was not excited by 500-nm radiation.

Pulsed excitation: lifetimes and time-resolved spectra

Room-temperature time-resolved emission spectra excited at 580 nm are shown in Fig. 5. As expected, the decay of the 780-nm broad band is fast compared to the decay of the R and N lines. The persistence of a broad tail (beyond 750 nm) at long times should be noted. Some of this tail remains even after the N lines have disappeared. Apparently, some of the broad emission is long-lived at room temperature. The spectra of the fast and slow broad components are different; the fast component is red shifted. When the temperature is reduced to 77°K, the overlapping of the broad band and line emission is reduced (Fig. 6) and the long-lived broad emission is no longer detectable. The assignments of the R- and N-line sidebands, as well as the correlation between the broad band and 731-nm line, are confirmed by the time-resolved spectra. The spectra in Figs. 5 and 6 were not corrected for wavelength variation

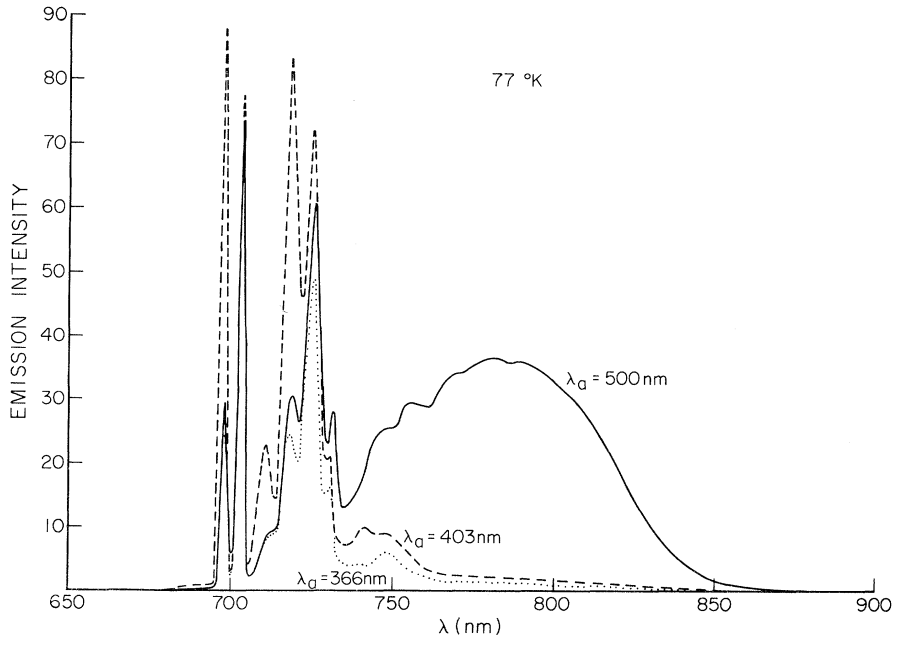

FIG. 2. Steady-state 77°K emission spectra of MgO: Cr^{3+} ($Cr^{3+} < 10^{18} cm^{-3}$) at different excitation wavelengths (λ_a).

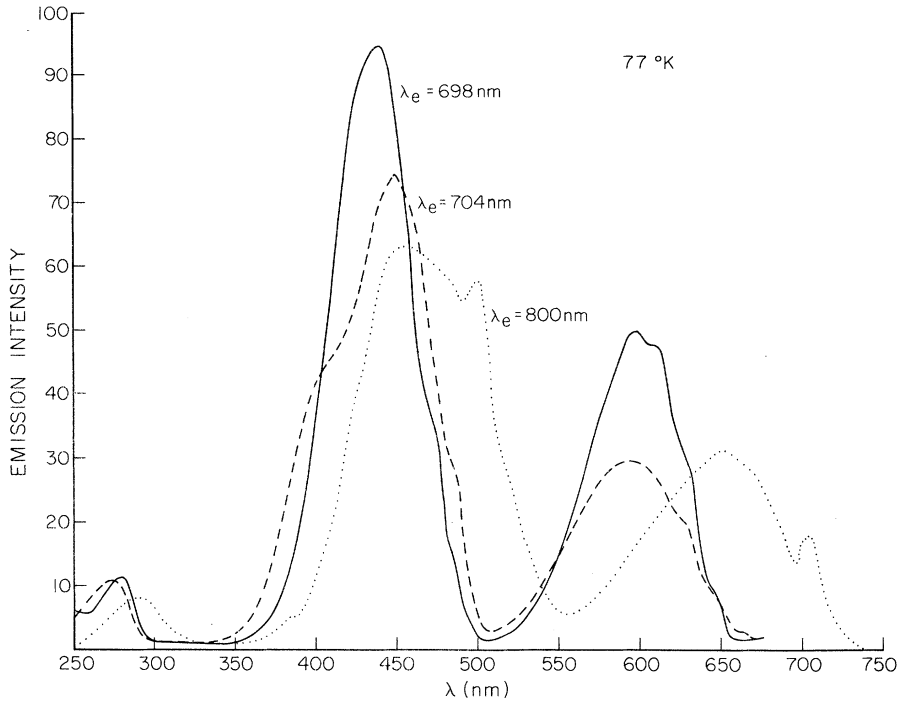

FIG. 3. Steady-state 77°K excitation spectra of MgO: Cr^{3+} ($Cr^{3+} < 10^{18} cm^{-3}$) at different monitoring wavelengths (λ_e).

of the detector sensitivity, but the spectral shapes in Figs. 5(b) and 6(b) are quite reliable since the response of the RCA C31034 detector used for these spectra is fairly flat in the region of interest.

In measuring the lifetimes of different portions of the emission spectrum, the excitation wavelength was chosen to minimize the overlapping of emissions of differing lifetimes. For instance, the R-line decay was measured with 580-nm excitation whereas the N-line decay was excited at 366 or 337 nm. The lifetime results are collected

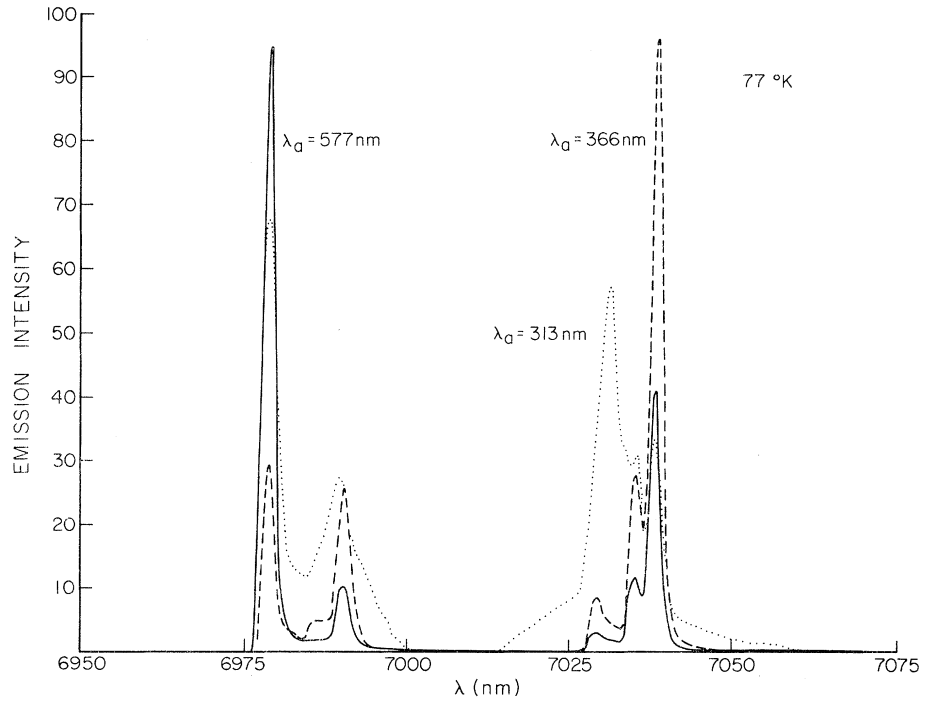

FIG. 4. High-resolution steady-state emission spectra (77°K) of MgO:Cr^{3+} ($Cr^{3+} < 10^{18} cm^{-3}$) at different excitation wavelengths (λ_a).

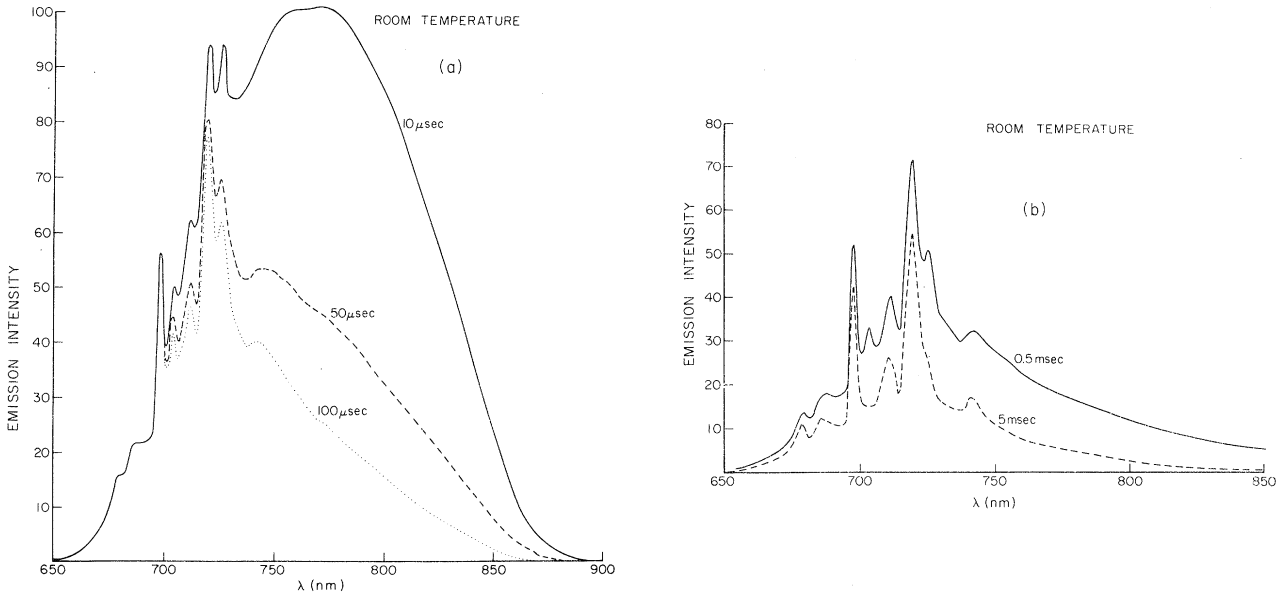

FIG. 5. Room-temperature time-resolved emission spectra of MgO:Cr^{3+} ($Cr^{3+} < 10^{18} cm^{-3}$) at different times after excitation. Excitation wavelength 580 nm.

in Table I. At room temperature the overlap of the broad fluorescence and the line emission led, at all monitoring wavelengths, to a multiexponential decay in which a fast component (35 μsec) was superimposed on slower decays. At 77°K, the narrowing of the broad-band emission reduces the spectral overlap to the point where the fast component is absent and single exponential decays are obtained when either the R or N lines are monitored.

Although lowering the temperature reduces the width of the broad-band emission, the peak intensity of the broad band is nearly the same at room temperature and at 77°K. Thus, the intensity of the 35-μsec component is not very sensitive to temperature. This was also found in the steady-

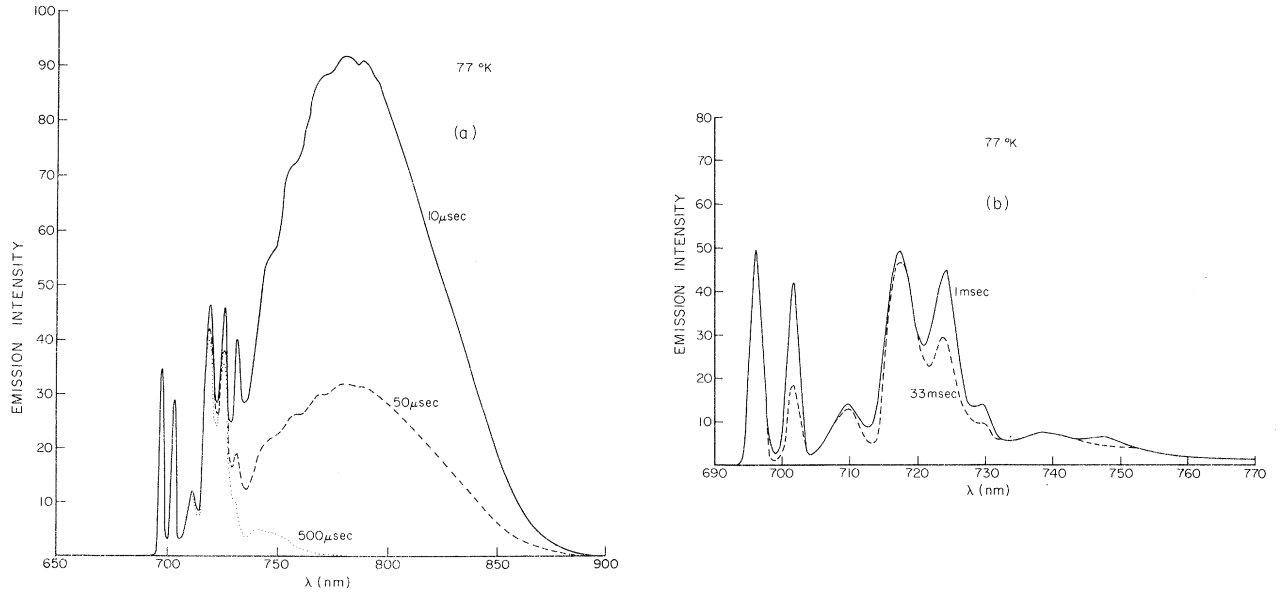

FIG. 6. Time-resolved 77°K emission spectra of MgO:Cr^{3+} ($Cr^{3+} < 10^{18} cm^{-3}$) at different times after excitation. Excitation wavelength 580 nm.

state emission whenever the broad band was a substantial part of the emission spectrum. Within the precision of our measurements, the 35-μsec lifetime is independent of temperature.

In the lifetime measurements it was not possible to resolve the two N lines at 7035 and 7038 Å. However, the high-resolution steady-state emission spectra show that the 7038-Å line is at least three times more intense than the 7035-Å line at the excitation wavelengths used, and the measured lifetimes at 704 nm reflect the decay of the 7038-Å line. With this proviso, the measured R- and N-line lifetimes at 77°K are in good agreement with those previously obtained.[4]

Time-resolved 77°K emission spectra excited at 580 nm [Fig. 6(b)] can be used to measure η, the ratio of the no-phonon line intensity to total emission from ^2E for the several centers. The 1-msec spectrum contains contributions from both cubic and tetragonal sites, whereas the emission from cubic sites dominates the 33-msec emission. The detection system (dilute chromium acetylacetonate solution filter, monochromator and RCA C31034 photomultiplier) was calibrated with a standard quartz-iodine lamp and the areas of the different bands in Fig. 6(b) were corrected before computing η. The corrected ratios are $\eta_R = 1/5.4$ and $\eta_N = 1/4.9$. If no corrections are applied to the areas, both values are ~10% smaller. The quantities are somewhat smaller than reported by Imbusch *et al.*,[4] but the use of time-resolved spectra permits a more direct estimation of η_R and η_N. The resolution of the overlapping R- and N-line vibronic sidebands was made by comparing the time-resolved spectra as a function of time and excitation wavelength. Within 10%, the same η values were found for both the 1- and 33-msec spectra. In this time interval the N emission intensity decreases by a factor of 2.7 compared to the R emission intensity.

The rise time of the long-lived emission was monitored at 698 nm with 580-nm excitation at 77°K. The monochromator slits were opened to 5 mm instead of the usual 0.5 mm, and some scattered laser light reached the detector. Within the resolution time of the apparatus under these conditions (200 nsec), no rise time was detected. Interference from the 35-μsec component was negligible.

A search for fluorescence components faster than 200 nsec has also been made. At room temperature, where no Dewar was required, a saturated solution of chromium acetylacetonate as a filter eliminated most of the scattered light in the 730–900-nm region, with no slits on the emission monochromator (~10-mm slit width), but the R- and N-line emission was partially absorbed by the filter solution. The time dependence of th · 750-nm emission is shown in Fig. 7 for different s weep rates. No component faster than ~35 μsec was detected; the rise times in the 10- and 50-nsec curves reflect the duration of the excitation pulse. The broken line in Fig. 7 illustrates the effect of scattered laser light, obtained when 698 nm is monitored. That this "fast" component is due to scattered light is demonstrated by its strong dependence on crystal position. A similar feature would be produced by prompt fluorescence with a short lifetime (see Sec. IV).

TABLE I. Lifetimes at different emission wavelengths.

Monitoring wavelength (nm)	Room temperature	77 °K
698 (R)	1.5 msec	11.6 msec
704 (N)	0.61 msec	8.6 msec
800 (broad band)	35 μsec 0.61 msec 1.5 msec	35 μsec

IV. DISCUSSION

Origin of the broad-band emission

The lifetime measurements and the time-resolved spectra show that at room temperature there are three different overlapping emissions (35 μsec,

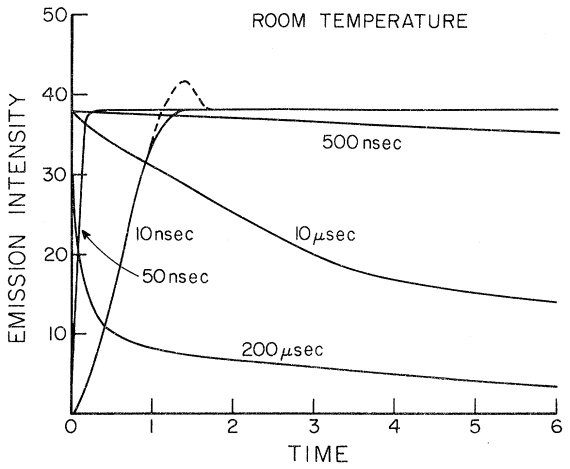

FIG. 7. Time evolution of the 750-nm emission of MgO:Cr^{3+} ($Cr^{3+} < 10^{18} cm^{-3}$) at room temperature and different excitation sweep rates with excitation at 580 nm. The time associated with each curve represents the magnitude of one division on the time coordinate. The broken line superimposed upon the 10-nsec profile illustrates the change introduced by monitoring 698-nm emission and indicates the effect of scattered laser light.

0.61 and 1.5 msec) in the broad-band region of the spectrum (800 nm). At 77°K only the 35-μsec component remains. The fast emission cannot be prompt fluorescence ($^4T_2 \rightarrow {}^4A_2$) from either the cubic or the tetragonal (single-ion or pair) centers for the following reasons.

(i) The activation spectrum at 77°K is completely different for the broad band than for either the R or the N lines.

(ii) No rise time for either the R or N lines, corresponding to a 35-μsec $^4T_2$ decay is observed.

(iii) The intensity ratio, broad band to lines, increases with concentration.

Since the N lines have been ascribed to the single-ion and pair-tetragonal sites, we assign the fast component to the rhombic sites which have been detected in the ESR spectra. The red shift in the excitation spectrum may be due to a lowering of Dq produced by the movement of O^{--} toward the vacancy.

The no-phonon lines of the $^4T_2 \rightarrow {}^4A_2$ transition have not been definitely identified for either the cubic or tetragonal spectra, but inspection of the $^4T_2 \leftarrow {}^4A_2$ absorption and excitation spectra band maxima indicates that $^4T_2$ lies about 2500 cm^{-1} above ^2E for these sites.[6] Since the half-width of the $^4T_2 \leftarrow {}^4A_2$ band is some 1700 cm^{-1}, the no-phonon level of $^4T_2$ is approximately 800 cm^{-1} above ^2E for both the cubic and tetragonal centers. The $^4T_2 \leftarrow {}^4A_2$ excitation spectrum for the broad-band emission from rhombic sites is markedly red shifted from the cubic and tetragonal spectra, and the $^4T_2$ origin in the rhombic system is about 1300 cm^{-1} lower than the corresponding level in the cubic centers. Since neither rhombic distortions nor changes in Dq will affect the ^2E energy appreciably, it appears that $^4T_2$ is below ^2E in the rhombic site species. The temperature variation of the broad-band intensity can now be readily understood. At 77°K only rhombic $^4T_2 \rightarrow {}^4A_2$ emission occurs; 35 μsec is a reasonable lifetime value for a spin-allowed transition in a Cr^{3+} system.[7] As the temperature is increased, delayed or equilibrium fluorescence is thermally activated and broad-band emission from both cubic (1.5 msec) and tetragonal (0.61 msec) sites is superimposed upon the "prompt" rhombic fluorescence. The $^4T_2$ states of the cubic and tetragonal sites are not repopulated at 77°K and the long-lived broad fluorescence is absent at low temperatures.

Thermal quenching of the R-line lifetime

Imbusch attributed the reduction of the R-line lifetime from 11.6 msec at 77°K to 1.5 msec at room temperature to an increase in the radiative $^2E \rightarrow {}^4A_2$ rate due to enhancement of the vibrational sidebands.[5] Di Bartolo and Powell[8] fitted the measured R-line lifetime (τ) to the equation

$$\tau^{-1} = \tau_i^{-1} + \tau_j^{-1} e^{-\Delta E_{ij}/kT}, \tag{1}$$

with $\tau_j = 36.8$ μsec and $\Delta E_{ij} = 834$ cm^{-1}. If ΔE_{ij} is interpreted as the ^2E-$^4T_2$ energy gap, the quenching of ^2E would proceed via $^4T_2$ in contrast to the conclusion of Imbusch. Di Bartolo and Powell found a similar energy gap (891 cm^{-1}) could be used to explain the thermal broadening of the R line by a phonon absorption mechanism, but regarded the agreement as fortuitous and rejected the involvement of $^4T_2$ in both the thermal-quenching and line-broadening processes because of the apparent disparity between the $^4T_2 \rightarrow {}^4A_2$ and $^2E \rightarrow {}^4A_2$ lifetimes. However, if the fast and slow decays originate in different centers, this argument is not pertinent and the involvement of $^4T_2$ in the thermal quenching of the cubic site emission must be reconsidered.

The importance of $^4T_2$ in the thermal relaxation pathway for ^2E states has been identified as an important mechanism in ruby,[9] emerald,[9] and other Cr^{3+} systems,[10] and the appearance of thermally activated broad-band emissions with the same lifetimes as the R and N lines indicates a similar mechanism for cubic and tetragonal centers in MgO:Cr^{3+}. The ratios of the R and N lines to the respective vibronic sideband intensities (η_R and η_N) are nearly independent of temperature. Clearly the ΔE_{ij} value of 834 cm^{-1} for the R-line temperature dependence is quite reasonable for the $^4T_2$-^2E separation and we suggest that repopulation of $^4T_2$ is the dominant pathway for the thermal relaxation of ^2E in cubic and tetragonal sites. If the delayed fluorescence and the R-line sidebands are not distinguished, the computed thermal enhancement of the $^2E \rightarrow {}^4A_2$ radiative rate will appear to account for the decrease in R-line lifetime as found by Imbusch,[5] but when the fluorescence contribution is subtracted from the total emission the radiative rate does not change very much with temperature.

$^4T_2$ lifetime and intersystem crossing efficiency (Φ_{2_E})

The rise time of the R-line emission is faster than 200 nsec and therefore the lifetime of $^4T_2$ is less than 200 nsec for cubic site ions. Although we have not been able to measure the $^4T_2$ lifetime directly, an upper limit for this quantity can be estimated from the emission monitored at 750 nm (Fig. 7), a wavelength where only broad-band fluorescence (prompt and delayed) is emitted.

The most conservative lifetime limit can be obtained by comparing the 77°K and room-temperature 750-nm decay curves. At 77°K, laser light

scattered by the Dewar could not be completely eliminated. This leads to a curve similar to the 10-nsec profile in Fig. 7, including the broken line "bump." If we assume that the $^4T_2$ lifetime is shorter than the measured excitation pulse width, a bump identical to that produced by scattered light would be seen. The height of this bump above the 35-μsec signal ($I^{\circ}_{\max}$) is proportional to $I_{\text{abs}} k_r \tau/\Delta$, where Δ is the excitation pulsewidth (10 nsec) and k_r the radiative $^4T_2 \rightarrow {}^4A_2$ rate. Since the 35-μsec intensity is independent of temperature, this signal can be used to relate $I^{\circ}_{\max}$ at 77°K and $I_{\max}$, the delayed fluorescence intensity measured about 100 μsec after excitation at room temperature. $I_{\max}$ is proportional to $I_{\text{abs}} k_{2_E} k_r \tau (3e^{-\Delta E/kT})$, where k_{2_E} is the $^4T_2 \rightarrow {}^2E$ intersystem crossing rate and the term in parentheses is the Boltzmann factor for equilibration between $^4T_2$ and ^2E. Since the proportionality factors in both $I^{\circ}_{\max}$ and I are the same and $\Delta E \simeq 800$ cm^{-1}

$$I_{\max}/I^{\circ}_{\max} = 6\times 10^{-10} k_{2_E} .$$

Experimentally, $I_{\max}/I^{\circ}_{\max} \geq 1$. Therefore, $k_{2_E} \geq 2\times 10^9 \text{sec}^{-1}$. Since $k_r \approx 10^5 \text{sec}^{-1}$, the 36.8 μsec(τ_f) value obtained with Eq. (1) implies that nonradiative decay from $^4T_2$ to $^4A_2$ is not very large and that $\tau = 1/k_{2_E}$. Consequently, $\tau \leq 0.5$ nsec. In all likelihood τ is smaller than 0.5 nsec because the $I^{\circ}_{\max}$ varies with crystal orientation and certainly contains some scattered light contribution.

If τ were between the 200 nsec limit obtained directly from the rise time and 0.5 nsec computed above, the prompt fluorescence signal would persist longer than does the observed bump.

The above discussion applies to the cubic and tetragonal centers where $^4T_2$ is above ^2E. In these sites $\Phi_{2_E} = 1$. In the rhombic centers, where $^4T_2$ is below ^2E, τ is governed by the relaxation rates from $^4T_2$ to $^4A_2$ and not by k_{2_E}. Hence the much longer $^4T_2$ lifetime (35 μsec) for the rhombic ions.

One of the aims of the present work was to determine the effect of the $^4T_2$-^2E separation on k_{2_E}. Attempts have been made to estimate this quantity from the rise times at 77°K of $^2E \rightarrow {}^4A_2$ emission in crystalline samples of $NaMgAl(C_2O_4)_3 \cdot 9H_2O:Cr^{3+}$, $Al_2O_3:Cr^{3+}$, and $Cr(urea)_6(ClO_4)_3$. In the first two of these materials, the $^4T_2$-^2E separation is undoubtably larger than the corresponding interval in either the cubic or tetragonal sites of $MgO:Cr^{3+}$, while in the last system it may be smaller.[10,11] Rise-time measurements have also been made at 77°K for glassy solutions of $Cr(CN)_6^{3-}$ and chromium acetylacetonate, molecules where the $^4T_2$-^2E separation is large.[10] In none of these cases was a rise time (> 1 nsec) detected, which means that $k_{2_E} \geq 10^9 \text{sec}^{-1}$. Consequently, in efforts to evaluate k_{2_E} from the $^4T_2$ lifetime a subnanosecond detection system must be employed.

Quantum yields

At low Cr^{3+} concentrations energy transfer between different types of centers is negligible as shown by the exponential decays of the R, N, and broad-band emissions at 77°K. This conclusion is also supported by the different excitation spectra for the different centers. Under the condition that no energy transfer takes place, the absolute quantum yield of $^2E \rightarrow {}^4A_2$ emission for each center can be expressed as

$$\Phi = \Phi_{2_E}(\tau/\tau_0),$$

where τ_0 is the radiative lifetime (including sideband contribution). As shown above, $\Phi_{2_E} \simeq 1$ for the cubic and tetragonal centers. The absorption strength ($\int \sigma d\nu$) of the R line has been measured as $(1.8\text{–}2.3)\times 10^{-20}$ cm^4 and calculated as 2.55×10^{-20} cm.[12] The latter value leads to $\tau_0^R = 85 \times 10^{-3}$ sec and $\tau_0 = \tau_0^R \eta_R = 16\times 10^{-3}$ sec, which, when compared to the low-temperature R-line lifetime of 11.5×10^{-3} sec, corresponds to $\Phi_{2_E \rightarrow {}^4A_2} = 0.72$. The deviation from unity would be somewhat larger if the experimental absorption strength were used in the computation of τ_0^R. The temperature independence of the total emission with temperature for very dilute crystals[5] suggests that $\Phi = 1$ for the cubic center. The same approach, when applied to the tetragonal centers, gives $\tau_0 = 40 \times 10^{-3}$ sec and $\Phi = 1.05$.

The measured lifetime of the rhombic center fluorescence is closely consonant with the natural lifetime computed from $^4T_2 \rightarrow {}^4A_2$ absorption bands and with the measured fluorescence lifetimes for systems with $^4T_2$ below ^2E (10–50 μsec).[7,13] It thus appears that the luminescence quantum yield for $^4T_2 \rightarrow {}^4A_2$ emission is unity for the rhombic centers. This conclusion is also supported by the temperature invariance of the fast lifetime.

Assignment of the 7031-Å line

This line, which is about as strong in absorption as the N lines,[4] is not found in emission excited by direct population of $^4T_2$ or $^4T_1$. Imbusch *et al.*[4] suggested that the 7031-Å line is due to a $^2E \rightarrow {}^4A_2$ transition in a rhombic center and that fluorescence is absent in emission because the greater strain sensitivity of rhombic site ions leads to preferential $^4T_2 \rightarrow {}^4A_2$ emission. The failure in detecting the 7031-Å line in the 77°K emission spectrum excited at 500 nm, a wavelength which is most effective for exciting the broad rhombic site fluorescence, would be expected if rapid vibrational relaxation takes place in $^4T_2$ since $^4T_2$

is below ^2E in the rhombic ions. The relatively high emission intensity of 7031 Å upon 313-nm excitation would then, in this interpretation, result from some intersystem crossing to doublet states when the higher-energy radiation is absorbed. Of course, the possibility that the 7031-Å line and the broad fluorescence originate in different centers cannot be excluded by our results.

V. CONCLUSIONS

The broad-band emission in $MgO:Cr^{3+}$ contains three components: fast prompt fluorescence from rhombic centers, and delayed fluorescence from cubic and tetragonal centers. In the cubic and tetragonal centers $^4T_2$ is above ^2E, the $^4T_2$ lifetimes are less than 0.5×10^{-9} sec, and only delayed fluorescence is observed at room temperature. In the rhombic sites $^4T_2$ is below ^2E and prompt fluorescence is emitted with a lifetime of 35 μ sec at both 77°K and higher temperatures.

The thermal relaxation of the R lines arises from the repopulation of $^4T_2$ rather than from an enhanced vibronic decay mechanism.

The absolute luminescence quantum yields appear to be unity for all the centers.

ACKNOWLEDGMENTS

We are very grateful to Dr. G. Imbusch for providing the $MgO:Cr^{3+}$ crystals that made this study possible and to Dr. G. K. Vemulapalli for making the 0.75-m Jarrell-Ash spectrometer system available to us.

---

*Permanent address: Istituto di Chimica Generale, Università di Roma, Roma, Italy.

†Research supported by the National Science Foundation Grant No. GP20120.

[1]J. H. Parker, Jr., R. W. Weinert, and J. G. Castle, Jr., in *Optical Properties of Ions in Crystals*, edited by H. M. Crosswhite and H. W. Moos (Wiley, New York, 1967), p. 251.

[2]S. Sugano, A. L. Schawlow, and F. Varsanyi, Phys. Rev. 120, 2045 (1960).

[3]G. F. Imbusch, A. L. Schawlow, A. D. May, and S. Sugano, Phys. Rev. 140, A830 (1965).

[4]J. P. Larkin, G. F. Imbusch, and F. Dravnieks, Phys. Rev. B 7, 495 (1973).

[5]G. F. Imbusch, Stanford University report, 1964 (unpublished).

[6]W. M. Fairbank, Jr. and G. K. Klauminzer, Phys. Rev. B 7, 500 (1973).

[7]M. L. Reynolds, W. E. Hagston, and F. J. Garlock, Phys. Status Solidi 30, 113 (1968).

[8]B. Di Bartolo and R. C. Powell, Nuovo Cimento B 66, 21 (1970).

[9]P. Kisliuk and C. A. Moore, Phys. Rev. 160, 307 (1967).

[10]F. Diomedi Camassei and L. S. Forster, J. Chem. Phys. 50, 2603 (1969).

[11]J. L. Laver and P. W. Smith, Aust. J. Chem. 24, 1807 (1971).

[12]R. M. Macfarlane, Phys. Rev. B 1, 989 (1970).

[13]L. Grabner, S. E. Stokowski, and W. S. Brower, Jr., Phys. Rev. B 2, 590 (1970).